International Journal of Automation and Computing 16(5), October 2019, 696-706
DOI: 10.1007/s11633-018-1132-0

Phenomenological Based Soft Sensor for Online Estimation of Slurry Rheological Properties

Jenny L. Diaz C.[1] Diego A. Muñoz[2] Hernan Alvarez[1]

[1] Research Group of Dynamic Processes, Universidad Nacional de Colombia-Sede Medellín, Facultad de Minas. Cra 80, Medellín 65-223, Colombia

[2] Mathematical Optimization of Processes, Centro de Ciencia Básica, Universidad Pontificia Bolivariana, Circular 1, Medellín 70-01, Colombia

Abstract: This work proposes a soft sensor based on a phenomenological model for online estimation of the density and viscosity of a slurry flowing through a pipe-and-fittings assembly (PFA). The model is developed considering the conservation principle applied to mass and momentum transfer and considering frictional energy losses to include the variables directly affecting slurry properties. A reported proposal for state observers with unknown inputs is used to develop the first block of the observer structure. The second block is constructed with two options for evaluating slurry viscosity, generating two possible estimator structures, which are tested using real data. A comparison between them indicates different uses and capabilities according to available process information.

Keywords: Soft sensor, phenomenological based semi-physical model, non-Newtonian fluids, unknown input observer, slurry flow.

1 Introduction

Slurries are the types of fluids predominant in industries like food, paper and mineral processing[1–4]. The transport of particles to or from size reduction or extraction processes implies operations with slurries in the plant. Material particles such as crystals or fibers are mixed with water, and eventually reagents to form a slurry. They are then processed, which strongly affects the slurry properties[5]. The majority of slurries exhibit non-Newtonian behavior and the properties and rheology of the suspension do not depend on only one parameter or process variable[6–8]. These properties are normally used as the quality indicator of the processed material. For instance, in distributed control of chemical networks, the distributed state estimation is a crucial thing to consider[9]. Therefore, to guarantee optimal operation, slurry properties must be correctly determined, measured, or estimated.

There are direct and indirect methods for characterizing the rheology of non-Newtonian fluids in each particular processing industry[10, 11]. The direct methods consist of using off-line techniques to determine slurry rheology (e.g., in laboratory), while the indirect methods use the available information of other measured variables from slurry processing or transport to estimate the slurry properties, for instances, the software sensors (soft sensors). In this case, soft sensors have been designed based on empirical models[2, 6, 11, 12], which provide poor information about the phenomenology of the process. Those empirical models are not generalized with other similar processes because they strongly depend on installation particularities and the kind of slurry being studied. Indeed, the phenomena that influence the slurry rheology are not explicitly considered for the construction of an empirical model. Therefore, the estimation of slurry properties using soft sensor based on empirical modeling is difficult when there are changes in process inputs, or when changes in phase properties modify slurry rheology. If the main factors affecting the properties of the mixture are known, the viscosity, as interesting rheological property, can be determined through a soft sensor, using a model based on phenomenology[13, 14]. This kind of model allows an explanation of the dependence of slurry properties on factors and parameters governing the slurry flow[15–18].

In this work, we propose an online estimation of rheological properties of slurries in general, including three key elements. The first one is the detailed development of a phenomenological based semi-physical model (PBSM) for slurries flowing through a typical pipe-and-fittings assembly. Current available models of this process do not allow the construction of the required observer, because of their static character or their inadequate mathematical structure. The second one is the incorporation of the PBSM into online observation of slurry density using commonly available measurements: flow rate and pressure. The third one, and also the main contribution of

Research Article
Manuscript received December 7, 2017; accepted April 25, 2018; published online September 3, 2018
Recommended by Associate Editor Jyh-Horng Chou

this work, is the way in which the main disturbance (the unknown input) was added to the model, and the estimation of two different viscosity calculation blocks to estimate both slurry properties. In particular, this work focuses on mineral slurries, but the proposed procedure is applicable to other industrial processes using this kind of fluid. We want to point out that the term observer is used for the known structure for state estimation[19, 20], and the term estimator is used for structure as a whole, containing one or more observers inside.

The paper is organized as follows. In Section 2, the proposed model for the flow process of a slurry through a pipe-and-fittings assembly (PFA) is explained in detail and the estimation structure is described and characterized. In Section 3, the two estimator proposals are applied to a real mineral processing process located in Colombia. Simulation results using the PBSM of the process as the plant and the estimator structures as soft sensor for slurry viscosity and density are shown. This paper closes with some brief conclusions in Section 4.

2 Estimation structure for density and viscosity of a slurry

One requirement for proposing a soft sensor is to have a model of the process where relations between measured variables and those variables to be estimated are explicit. Models for slurry flow in pipelines are available in the literature, some are simple[16], and others are more complex[21, 22]. However, due to the static character and non-explicit form of those process variables which affect rheological properties, e.g., density and viscosity, these models do not allow to be considered as structure for a soft sensor. Therefore, a phenomenological based semi-physical model is developed here, using the methodology proposed[14, 23].

2.1 Model of a slurry flowing through a PFA

Let us consider a pipe-and-fitting assembly (PFA) where a mineral slurry is transported from one process unit to another, as shown in Fig. 1. The intention is to estimate slurry density and viscosity using the available measurements in the PFA section: inlet pressure, P_1, outlet pressure, P_2, pressure transmitters (PT1 and PT2), and volumetric flow rate of the slurry, Q, and flow transmitter (FT). For this model, the following assumptions are considered:

1) The slurry is a mixture of water with solids, without chemical reactions taking place, and with no heat exchange with surroundings.

2) The concentration of solids in the mixture at inlet point is an unknown input.

3) The fluid suffers energy losses due to friction between fluid and pipe walls, and between fluid portions in contact during the flow.

4) For the vertical pipeline section, a turbulent flow regime is considered to avoid sedimentation of solids.

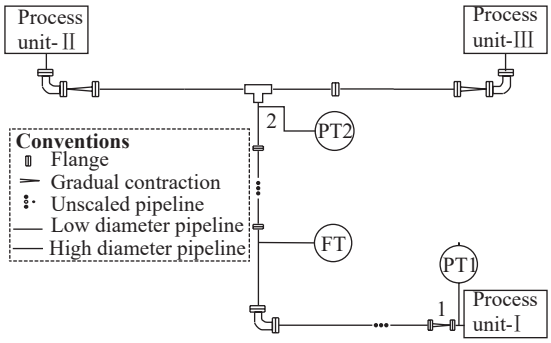

Fig. 1 Flowsheet of a pipe-and-fittings assembly to transport a slurry from process units I to II. PT1 and PT2 are pressure transmitters and FT is a flow transmitter.

Based on the above and according to the methodology for developing a PBSM, a process systems block diagram for selected PFA section is illustrated in Fig. 2. Two process systems (PS) are required to identify the interactions causing energy losses, which are detected as a pressure drop in the pipeline. The process system I (PS-I) represents the slurry contained in the selected section of the PFA with the same internal volume. The process system II (PS-II) represents the mass of pipe and the fittings forming the selected PFA section. PS-II is considered to be a sump for the mechanical energy lost during slurry flow through the PFA, which is dissipated as noise and small amplitude mechanical vibrations to the surroundings. Equations for PS-II are not presented here due to its simple role and poor contribution to the model.

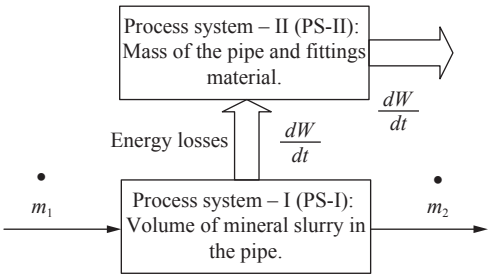

Fig. 2 Process systems used for modeling the slurry flow through the PFA section. PS-I represents the slurry contained in the selected section of the PFA. PS-II represents the mass of pipe and the fittings forming the selected PFA section.

Considering only the PS-I, the next model equations are formulated applying the principle of conservation of mass and energy.

Total mass balance.

$$\frac{\mathrm{d}M}{\mathrm{d}t} = \dot{m}_1 - \dot{m}_2 \tag{1}$$

where M is the total mass of slurry into the PFA section, and $\dot{m}_1$ and $\dot{m}_2$ are the inlet and the outlet mass flow of the slurry, measured at the same positions of pressure transmitters PT1 and PT2. Replacing total mass and mass flows in terms of total volume, V, inlet and outlet densities, ρ_1, ρ_2, and volumetric flow, Q, we get the next equation for outlet density changes:

$$\frac{\mathrm{d}\rho_2}{\mathrm{d}t} = (\rho_1 - \rho_2)\frac{Q}{V}. \tag{2}$$

Note that, at each stationary state, Q has the same value at inlet and outlet points due to slurry incompressibility. However, when an unknown disturbance occurs, i.e., the inlet content of solids changes, the slurry density also changes and a transition from one stationary point to another of Q is carried out. Additionally, $\dot{m}_2$ can be different due to the homogenization of any change of inlet content of solids.

Total energy balance. For a slurry flowing through a PFA, the changes in kinetic energy can be described by the following general equation:

$$\frac{1}{2}\frac{\mathrm{d}(M_P v^2)}{\mathrm{d}t} = W_f + W_g + W_{fr} \tag{3}$$

where v is the flow velocity and W_f, W_g and W_{fr} are the flow, gravitational, and friction works acting on the fluid, respectively. No driving machine work was included and only the effect of gravity was considered as external forces field action. Each one of these terms can be represented as follows:

$$W_f = -\left(\frac{\dot{m}_2}{\rho_2}P_2 - \frac{\dot{m}_1}{\rho_1}P_1\right) \tag{4}$$

$$W_g = -g\left(\dot{m}_2 z_2 - \dot{m}_1 z_1\right) \tag{5}$$

$$W_{fr} = -\dot{m}_1 h_{f_{1\to HP}} - \dot{m}_2 h_{f_{HP\to 2}} \tag{6}$$

where g is gravity, z_1 and z_2 are the height at the inlet and outlet with respect to a reference, respectively, and $h_{f_{1\to HP}}$ and $h_{f_{HP\to 2}}$ are the friction losses from inlet to a homogenization point (HP), and from HP to outlet point, respectively. HP is located near Point 1 due to turbulent flow and it is arbitrarily chosen.

Expressing the total mass of the slurry as $M = \rho_2\, A\, L$, with A and L being the pipe cross area and pipe length, and remembering that the mass flow is equal to $\dot{m}_2 = \rho_2 A v$, the equation for volumetric flow variations is

$$\frac{\mathrm{d}Q}{\mathrm{d}t} = \frac{A}{L}\left(-\frac{P_2}{\rho_2} + \frac{\dot{m}_1}{\dot{m}_2}\frac{P_1}{\rho_1} - g z_2 + \frac{\dot{m}_1}{\dot{m}_2} g z_1 - \frac{\dot{m}_1}{\dot{m}_2} h_{f_{1\to HP}} - h_{f_{HP\to 2}}\right). \tag{7}$$

All variables, including density, could change between Points 1 and 2 due to the dynamic behavior of the slurry when changes in inlet concentration or flow take place. We want to point out that such a variation takes place due to changes in the content of solids in spite of the incompressibility of the slurry. This fact is the main contribution of a PBSM for a soft sensor construction, as will be shown in Section 2.2. The model structure is formed by (2) and (7), which have valuable information for the model. A summary with the model variables, parameters and constants is provided in Table 1.

Table 1 Model variables, structural parameters, and structural constants

	PS-I	Total
Variables	ρ_2, Q	2
Parameters	A, L, V, P_1, P_2, $\dot{m}_1$, $\dot{m}_2$, ρ_1, z_1, z_2, $h_{f_{1\to HP}}$, $h_{f_{HP\to 2}}$	12
Constants	g	1

Known values from PFA, A, L, V, z_1, z_2, and operation conditions, P_1, P_2 act as trivial constitutive equations. For the remaining parameters, the constitutive equations are summarized in Table 2.

Note that until now, there is no equation (algebraic or differential) for calculating the outlet slurry viscosity, μ_2, which is one of the unknown variables to be estimated. The only relation between density and viscosity is given by N_{Re_i}, strongly affecting $h_{f_{1\to HP}}$ and $h_{f_{HP\to 2}}$. This implies that viscosity is not a variable in the main model structure, which is a limitation when attempting to establish traditional observers for this slurry property. Additionally, according to Table 2, the inlet density is calculated using the inlet solids fraction, $w_{S,1}$, which is an unknown input.

2.2 Soft sensor structure

The estimation structure is formed by a state observer for both states, outlet density ρ_2 and flow rate Q, and a calculation block for outlet viscosity μ_2. In the estimator proposed here, the observation of flow rate Q is only used for internal adjustments of the estimation, because this variable is measured online. The computational block for μ_2 is required because the model does not have this viscosity as a state. Inlet properties, such as density, viscosity and the inlet solids fraction fraction are unknown. Three available measurements in plant, slurry flow rate and PFA inlet and outlet pressures, are used as known values. Proposed structure acts as a soft sensor, using the PBSM developed in Section 2.1 as the base for an unknown input observer (UIO) for ρ_2. Two options for the μ_2 computational block are proposed here, producing two approaches to estimator construction, which are illustrated in Fig. 3 and described in Section 2.2.2.

2.2.1 Unknown input observer

The unknown input observer (UIO) is a kind of ob-

Table 2 Constitutive equations for structural parameters

#	Description	Constitutive equation	Reference
1	Inlet density	$\rho_1 = \dfrac{1}{\dfrac{w_{W,1}}{\rho_W} + \dfrac{w_{S,1}}{\rho_S}}$	[24]
2	Inlet mass flow	$\dot{m}_1 = \rho_1 \, A \, v$	[16]
3	Outlet mass flow	$\dot{m}_2 = \rho_2 \, A \, v$	[16]
4	Velocity	$v = \dfrac{Q}{A}$	
4	Friction losses	$h_{f_{i\to j}} = (K_{P_k} + \Sigma K_{F_k}) \dfrac{Q^2}{2\,A^2}$	[16]
5	Energy losses factors for pipeline	$K_{P_k} = f_{D_k} \dfrac{D}{L}$	[16]
6	Energy losses factors for fittings	$K_{F_k} = \dfrac{K_{1,k}}{N_{Re_i}} + K_{\infty,k}\left(1 + \dfrac{1}{ID_k}\right)$	[25]
7	Darcy's friction factor	$f_{D_k} = \left\{-2\log\left[\dfrac{\frac{\epsilon}{D}}{3.71} - \dfrac{5.02}{N_{Re_i}}\log\left(\dfrac{\frac{\epsilon}{D}}{3.71} + \dfrac{14.5}{N_{Re_i}}\right)\right]\right\}^{-2}$	[26]
8	Reynolds number	$N_{Re_i} = \dfrac{\left(\frac{Q}{A}\right) D \, \rho_i}{\mu_i}$	[16]

where ρ_W and ρ_S are the water and average solid density, respectively, $K_{1,k}$ and $K_{\infty,k}$ are taken from a fitting table given in Hooper's work[25], ID_k is the pipe internal diameter of fitting in inches, and ϵ is the pipe roughness. Indexes: $i = 1$, HP; $j = HP$, 2; k enumerates the fitting.

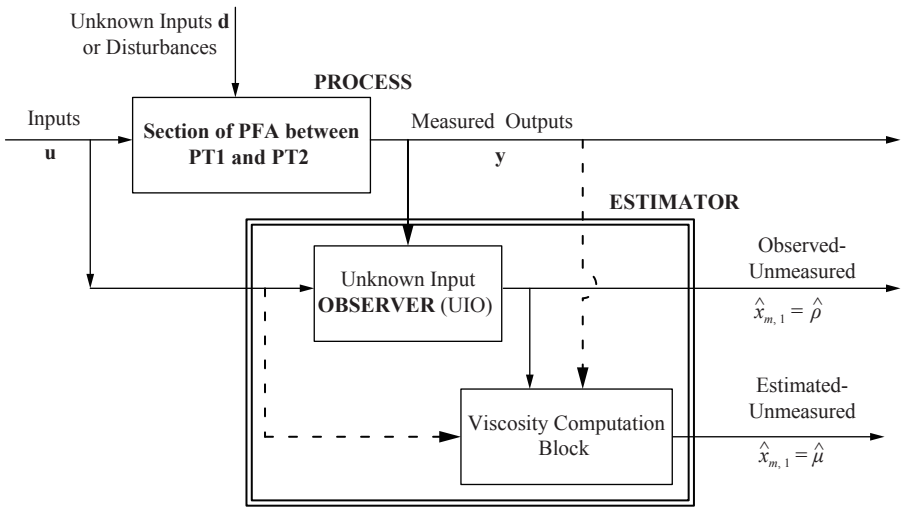

Fig. 3 Estimation structure: a state observer for ρ_2 and Q and a viscosity computation block. For Option 1, viscosity computation block requires only the observed unmeasured variable, while for Option 2, system inputs and outputs are also required (dashed lines represent additional connections).

server based on a linearized version of the process model and its main requirement is the capability to separate the unknown inputs. Note that the implicit relation between density and viscosity in the Reynolds number avoids the use of nonlinear structures[27–29], which requires an explicit separability.

The model structure obtained from the previously exposed phenomenological approach, is fixed and known. In this case, for the proposed UIO the model basic structure is given by (2) and (7) and the variable definition is described in Table 3. This system is linearized using Taylor series expansion around the process operation point shown in Table 3. The design of the UIO follows the methodology proposed in [20], where the conditions of observability and existence are stated. A two-state nonlinear model (on the left) and linearized version of the mod-

Table 3 Classification of the process variables and their steady state values

Kind of variable	Vector	Steady state values
State variables:	$\boldsymbol{x} = [\rho_2, Q]$	$\boldsymbol{x}_{ss} = [104\,1\ \mathrm{kg/m^3}, 0.062\,4\ \mathrm{m^3/s}]$
Known inputs:	$\boldsymbol{u} = [P_1, P_2]$	$\boldsymbol{u}_{ss} = [0.487\ \mathrm{MPa}, 0.345\ \mathrm{MPa}]$
Unknown inputs:	$\boldsymbol{d} = [w_{S,1}]$	$\boldsymbol{d}_{ss} = [0.063\,9\ \mathrm{kg_{solids}/kg_{slurry}}]$
Measured outputs:	$\boldsymbol{y} = [Q]$	$\boldsymbol{y}_{ss} = [0.062\,4\ \mathrm{m^3/s}]$

el (to the right), are represented in state-space format as follows:

$$\begin{aligned} \dot{\boldsymbol{x}} = \boldsymbol{f}(\boldsymbol{x}, \boldsymbol{u}, \boldsymbol{d}) \quad &\rightarrow \quad \dot{\boldsymbol{x}} = \boldsymbol{A}\boldsymbol{x} + \boldsymbol{B}\boldsymbol{u} + \boldsymbol{D}\boldsymbol{d} \\ \boldsymbol{y} = \boldsymbol{h}(\boldsymbol{x}) \quad &\rightarrow \quad \boldsymbol{y} = \boldsymbol{C}\boldsymbol{x} \end{aligned} \tag{8}$$

where $\boldsymbol{x} \in X \subseteq \mathbf{R}^{n_x}, \boldsymbol{u} \in U \subseteq \mathbf{R}^{n_u}, \boldsymbol{d} \in D \subseteq \mathbf{R}^{n_d}$ and $\boldsymbol{y} \in \mathcal{Y} \subseteq \mathbf{R}^{n_y}$ are the state, manipulated input, unknown input and output vector, respectively. Moreover, $\boldsymbol{f} : \mathbf{R}^{n_x} \times \mathbf{R}^{n_u} \times \mathbf{R}^{n_d} \rightarrow \mathbf{R}^{n_x}$ and $\boldsymbol{h} : \mathbf{R}^{n_x} \rightarrow \mathbf{R}^{n_y}$ are the nonlinear mapping functions for the dynamics and output equations, respectively. $\boldsymbol{A} \in \mathbf{R}^{n_x \times n_x}$, $\boldsymbol{B} \in \mathbf{R}^{n_x \times n_u}$, $\boldsymbol{D} \in \mathbf{R}^{n_x \times n_d}$ and $\boldsymbol{C} \in \mathbf{R}^{n_y \times n_x}$ are matrices for unforced process response, forced process response due to known inputs, forced response due to unknown inputs taken as disturbances, and sensors conversion, respectively. The standard equations given in [20] to describe the dynamics of one UIO are

$$\dot{\boldsymbol{z}} = \boldsymbol{N}\boldsymbol{z} + \boldsymbol{L}\boldsymbol{y} + \boldsymbol{G}\boldsymbol{u} \tag{9}$$

$$\hat{\boldsymbol{x}} = \boldsymbol{z} - \boldsymbol{E}\boldsymbol{y} \tag{10}$$

where $\hat{\boldsymbol{x}}$ is the vector of estimated state, $\boldsymbol{z}$ is the vector of state transformation for observer design. $\boldsymbol{N} \in \mathbf{R}^{n_x \times n_x}$, $\boldsymbol{L} \in \mathbf{R}^{n_x \times n_y}, \boldsymbol{G} \in \mathbf{R}^{n_x \times n_u}$ and $\boldsymbol{E} \in \mathbf{R}^{n_x \times n_d}$ are the UIO matrices. These observer matrices must be selected to ensure convergence of the observer. Thus, based on the error dynamics given by

$$\boldsymbol{e} = \hat{\boldsymbol{x}} - \boldsymbol{x} = \boldsymbol{z} - \boldsymbol{x} - \boldsymbol{E}\boldsymbol{y} \tag{11}$$

the design is to determine matrices ensuring that the estimated state asymptotically converges to the real state value. Replacing the equations for linear model and linear observer in (11), the error dynamics can be expressed as

$$\dot{\boldsymbol{e}} = \boldsymbol{N}\boldsymbol{e} + (\boldsymbol{N}\boldsymbol{P} + \boldsymbol{L}\boldsymbol{C} - \boldsymbol{P}\boldsymbol{A})\,\boldsymbol{x} + (\boldsymbol{G} - \boldsymbol{P}\boldsymbol{B})\,\boldsymbol{u} - \boldsymbol{P}\boldsymbol{D}\boldsymbol{d} \tag{12}$$

where $\boldsymbol{P}$ is a matrix defined as

$$\boldsymbol{P} = \boldsymbol{I} + \boldsymbol{E}\boldsymbol{C} \tag{13}$$

with $\boldsymbol{I}$ a diagonal unitary matrix of order n_x, equal to the order of the model in state-space. If the matrices $\boldsymbol{E}$, $\boldsymbol{G}$ and $\boldsymbol{L}$ are calculated based on the following equations:

$$\begin{aligned} &\boldsymbol{P}\boldsymbol{D} = 0; \;\; (\boldsymbol{I} + \boldsymbol{E}\boldsymbol{C})\boldsymbol{D} = 0; \;\; \boldsymbol{G} = \boldsymbol{P}\boldsymbol{B} \\ &\boldsymbol{N}\boldsymbol{P} + \boldsymbol{L}\boldsymbol{C} - \boldsymbol{P}\boldsymbol{A} = 0 \end{aligned} \tag{14}$$

the error dynamics is reduced to

$$\dot{\boldsymbol{e}} = \boldsymbol{N}\boldsymbol{e}. \tag{15}$$

However, matrix $\boldsymbol{N}$ must satisfy the Hurwitz condition (eigenvalues with real part negative) for ensuring asymptotic convergence for error dynamics. Therefore, this matrix can be obtained from

$$\boldsymbol{N} = \boldsymbol{P}\boldsymbol{A} - \boldsymbol{K}\boldsymbol{C} \tag{16}$$

with the gain matrix calculated as

$$\boldsymbol{K} = \boldsymbol{L} + \boldsymbol{N}\boldsymbol{E} \tag{17}$$

where the entries of matrix $\boldsymbol{K}$ are selected to satisfy Hurwitz condition.

It is evident that knowing matrices $\boldsymbol{N}$, $\boldsymbol{L}$, $\boldsymbol{G}$ and $\boldsymbol{E}$, the state estimation $\hat{\boldsymbol{x}}$ is easily evaluated solving the dynamic system given by (9) and (10). All observer matrices must be selected to guarantee the following conditions of existence and observability. Taking the pair $(\boldsymbol{P}\boldsymbol{A}, \boldsymbol{C})$ into account, the observability matrix is given by

$$\boldsymbol{O} = \begin{bmatrix} \boldsymbol{C} \\ \boldsymbol{C}\boldsymbol{P}\boldsymbol{A} \\ \vdots \\ \boldsymbol{C}(\boldsymbol{P}\boldsymbol{A})^{n-1} \end{bmatrix}. \tag{18}$$

If the $\text{rank}(\boldsymbol{O}) = n_x$, the pair $(\boldsymbol{P}\boldsymbol{A}, \boldsymbol{C})$ will be observable, while for the opposite case, it will not be. When the pair $(\boldsymbol{P}\boldsymbol{A}, \boldsymbol{C})$ is not observable, the eigenvalues of $\boldsymbol{K}$ cannot be arbitrarily located and it is necessary to guarantee that the pair $(\boldsymbol{P}\boldsymbol{A}, \boldsymbol{C})$ is at least detectable. Next is the test of these conditions for the UIO design.

1) Existence condition: There exists a UIO if and only if the following equation is satisfied[20]:

$$\text{rank}(\boldsymbol{C}\boldsymbol{D}) = \text{rank}(\boldsymbol{D}) = n_d \tag{19}$$

with n_d being the dimension of the vector of unknown inputs.

2) Condition for the arbitrary error dynamics: If the observability of the system is not guaranteed, it is necessary to verify that the system is at least detectable. Thus, the following condition must be evaluated:

$$\text{rank} \begin{bmatrix} s\boldsymbol{P} - \boldsymbol{P}\boldsymbol{A} \\ \boldsymbol{C} \end{bmatrix} = n_x, \; \forall s \in \boldsymbol{C}. \tag{20}$$

For the steady state presented in Table 2, the linearized matrices for the observer design are

$$\boldsymbol{A} = \begin{bmatrix} -0.161\,4 & 0 \\ -0.000\,3 & -0.446\,5 \end{bmatrix}, \quad \boldsymbol{B} = \begin{bmatrix} 0 & 0 & 0 \\ 0 & 0 & -0.031\,4 \end{bmatrix}$$
$$\boldsymbol{C} = \begin{bmatrix} 0 & 1 \end{bmatrix}, \quad \boldsymbol{D} = \begin{bmatrix} 109.682\,7 \\ -0.006\,5 \end{bmatrix}.$$

Thus, for this linearized system, the existence condition, $\text{rank}(\boldsymbol{C}\boldsymbol{D}) = 1 = n_d \wedge \text{rank}(\boldsymbol{D}) = 1 = n_d$, and the detectability condition of the system

$$\text{rank} \begin{bmatrix} 4.722 & 8\,073.194 \\ 0 & 0 \\ 0 & 1 \end{bmatrix} = 2 = n_x$$

are satisfied. To fulfill the Hurwitz condition in matrix $\boldsymbol{N}$, the observer gains are fixed as follows:

$$\boldsymbol{K} = \begin{bmatrix} k_1 \\ k_2 \end{bmatrix} = \begin{bmatrix} -7\,020.5 \\ 4 \end{bmatrix}. \tag{21}$$

In this case, the value of k_1 is set equal to the component of the first row and second column of the matrix $\boldsymbol{PA}$ to cancel the same component in the resulting matrix $\boldsymbol{N}$. On the other hand, k_2 is a free value because the corresponding value in the matrix $\boldsymbol{PA}$, (16), is equal to zero, and k_2 is directly an element of the diagonal in the resulting matrix $\boldsymbol{N}$. From this, the matrix $\boldsymbol{N}$ is defined as

$$\boldsymbol{N} = \begin{bmatrix} -4.659\,5 & 0 \\ 0 & -4.000\,0 \end{bmatrix}. \tag{22}$$

With previous derivations, the eigenvalues of matrix $\boldsymbol{N}$ have negative real parts and the Hurwitz condition is satisfied. The other matrices for the observer can be calculated using the equations presented above, resulting in:

$$\boldsymbol{L} = \begin{bmatrix} 71\,518 \\ 0 \end{bmatrix} \tag{23}$$

$$\boldsymbol{G} = \begin{bmatrix} 0.044\,4 & -0.044\,4 & -529.026\,3 \\ 0 & 0 & 0 \end{bmatrix} \tag{24}$$

which complete the observer design.

2.2.2 Viscosity calculation block

1) The first option for the viscosity calculation block uses the non-Newtonian model for slurry viscosity. This option is very useful if a good characterization of rheological behavior of the slurry is available. In this case, the pseudoplastic behavior for volumetric concentrations is represented by the power law model:

$$\mu_2 = K_\mu |\dot{\gamma}|^{n-1} \tag{25}$$

where K_μ and n were identified using laboratory tests covering a wide range of shear stresses with different volumetric concentrations of solids in water[30], obtaining two polynomial correlations as a function of a solids fraction:

$$K_\mu = 981\,072 w_{s,1}^2 - 45\,397 w_{s,1} + 583 \tag{26}$$

$$n = -269.9 w_{s,1}^3 + 104.1 w_{s,1}^2 - 12.0 w_{s,1} + 0.62. \tag{27}$$

Thus, a formulation to calculate the slurry viscosity as a function of the solids fraction is available. In order to relate viscosity with operational conditions, for non-Newtonian fluids flowing through a pipeline, the shear stress can be computed using the following equation[31]:

$$\dot{\gamma} = \frac{3}{4}\left(\frac{8v}{D}\right) + \frac{1}{4}\left(\frac{8v}{D}\right)\frac{\mathrm{d}\left(\ln\left(\frac{8v}{D}\right)\right)}{\mathrm{d}\left(\ln\left(\frac{D\Delta P}{4L}\right)\right)} \tag{28}$$

where D and L are the diameter and length of the PFA, v is the slurry velocity in the line and the term $\frac{8v}{D}$ corresponds to the wall shear rate, while the term $\frac{D\Delta P}{4L}$ is the wall shear stress. For the case of fluids represented by the power law model, (25), the logarithm term can be replaced with the reciprocal of the exponent of the power law model and the wall shear rate can be determined by the following equation:

$$\dot{\gamma} = \frac{3n+1}{4n}\frac{8v}{D}. \tag{29}$$

Replacing (29) in (25), the slurry viscosity computation block as a function of the operation condition is

$$\mu_2 = K_\mu \left(\frac{3n+1}{4n}\frac{8v}{D}\right)^{n-1}. \tag{30}$$

Note that this option fails if the material being processed is changed, because the rheological model for viscosity could change, or its parameters may suffer dramatic variations not explicitly considered in the estimator. However, these changes are totally anticipated in any industrial facility.

2) The second option uses the mechanical energy balance in the stationary state between the inlet and outlet PFA section[32], i.e., $\frac{\mathrm{d}Q}{\mathrm{d}t} = 0$ in (7). Assuming that the slurry inside the pipeline is homogeneous through all the PFA, i.e., $\rho_1 = \rho_2 = \rho$ and $\dot{m}_1 = \dot{m}_2$, (7) becomes

$$0 = -\frac{P_2}{\rho} + \frac{P_1}{\rho} - g\, z_2 + g\, z_1 - h_{f_{1\to 2}}. \tag{31}$$

These considerations are valid because pressure changes are faster than solids fraction changes. Thus, at each iteration, the measured and estimated values are used for solving a system of one unknown variable (viscosity) and one equation (31), where the friction loss term $h_{f_{1\to 2}}$ depends implicitly on viscosity. A seed value for slurry viscosity is required for solving (31). This option can handle solid changes, i.e., variations in the slurry′s mineralogical composition, because it does not require experimental results for the treated slurry. Therefore, the structure can be applied independently of the slurry being processed, taking into account the fact that estimation precision is affected by the steady state assumption. However, for some applications, a low error is accepted because otherwise no measure would exist.

3 Estimator application and simulation results

To evaluate both estimation options, we consider step changes in the inlet solids fraction while maintaining the same pressure drop between the inlet-outlet of the PFA selected section. Estimator responses are obtained by

solving the process model and the estimator equations. Random noise is included in the measured variable to replicate the operation of real sensors. All simulations reproduce the operation at the constant pressure drop of current plant, because the model was validated with data from a real process. Additionally, a comparison with a nonlinear observer is discussed.

3.1 Performance of the estimation near the operating point

In this case, disturbances to the inlet solids fraction, shown in Fig. 4, are applied. Fig. 5 shows the slurry volumetric flow rate Q of the plant, represented by continuous black and gray lines for Options 1 and 2, respectively, and the two estimations for this variable, represented by dashed gray and light gray lines for Options 1 and 2, respectively. Two tests are considered to avoid excessive line overlap. It is important to note that state Q is measured, but the proposed structure uses its estimation to reconstruct unmeasured state ρ_2. The overlapping of the continuous black and gray lines in Fig. 5 shows that both

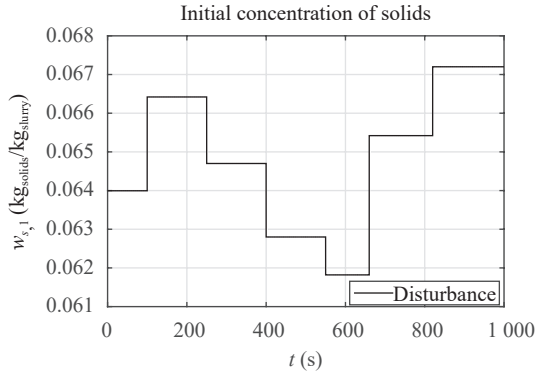

Fig. 4 Disturbances applied to the inlet solids fraction to the evaluate performance of estimation near the operating point

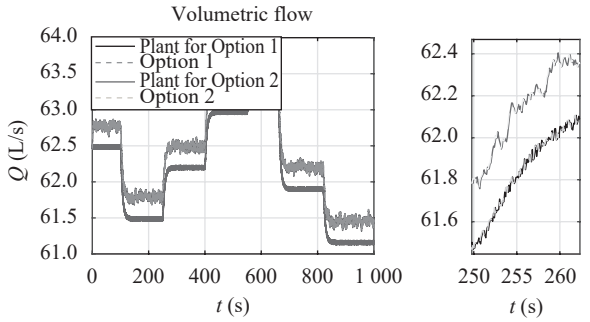

Fig. 5 Estimation of the volumetric flow of mineral slurry. Left: Volumetric flow observation using both estimation options and considering the disturbances applied to the inlet solids fraction shown in Fig. 4. Continuous black and gray lines represent the Q value of the plant for Options 1 and 2, respectively. Dashed gray and light gray lines represent the estimation value of Q for Options 1 and 2, respectively. Right: Close up of left figure for $t \in [250\text{ s}, 265\text{ s}]$.

options give nearly the same results for calculating Q, although Option 2 reflects a small amount of additional noise that was artificially added.

Figs. 6 and 7 show the observation of ρ_2 and μ_2, respectively. As expected, when the solids concentration at input increases, the slurry density and viscosity will also increase, while the volumetric flow decreases. This behavior is due to the higher energy requirement for transporting a slurry with higher solids content, and as the pressure drop remains constant, the transport capacity of the system for a heavier slurry is low. For Option 2, the estimation of the unmeasured variable is not as close as desired to the value of the plant compared to Option 1. However, as time passes and the system remains at the steady state, the precision of the Option 2 estimator will improve. Additionally, when one disturbance takes place, the estimation of the unmeasured variable with Option 2 will loses precision until the new steady state is reached. The effect of noise in Option 2 is higher than the effect in Option 1, due to the strong dependence of Option 2 on the steady-state condition, which is altered by inherent to real sensors noise.

Additionally, in order to have a numeric comparison of estimation quality between both estimator structures,

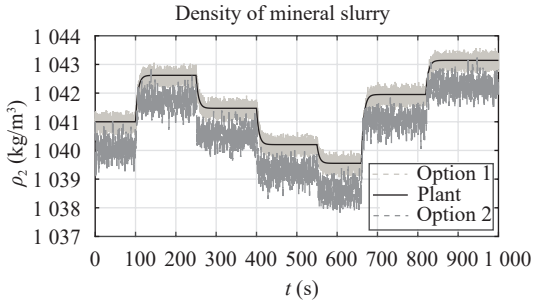

Fig. 6 Density observation using both estimation options and considering the disturbances applied to the inlet solids fraction shown in Fig. 4. Continuous black line represents the ρ_2 value of the plant. Dashed gray and light gray lines represent the estimation ρ_2 value for Options 1 and 2, respectively.

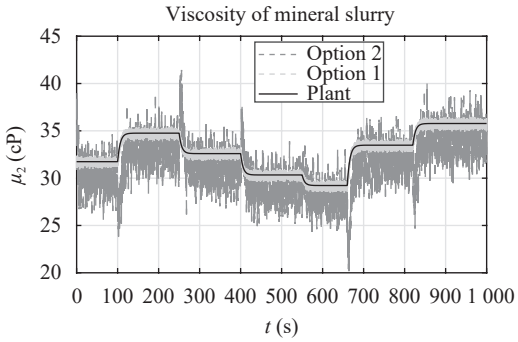

Fig. 7 Viscosity observation using both estimation options and considering the disturbances applied to the inlet solids fraction shown in Fig. 4. Continuous black line represents the value of μ_2 of the plant. Dashed light gray and dashed gray lines represent the estimation value of μ_2 for Options 1 and 2, respectively.

the integral time absolute error (ITAE) index is evaluated for each option. Results for previous simulations are presented in Table 4. Comparing the two proposed structures based on ITAE, it is evident that Option 1 performs better. The main difference in observed performance is on unmeasured variables, where Option 1 presents an ITAE lower than Option 2. Therefore, it is possible to obtain a better estimation when the slurry is characterized with previous experimental data. However, the less restrictive applicability of Option 2 allows its wide use taken into account its less precision and high noise sensitivity.

Table 4 ITAE index for the state estimation of the transport of a mineral slurry with noise

Variable	ITAE Option 1	ITAE Option 2
Q	334.3	346.9
ρ_2	162.1	891.3
μ_2	8385.7	58799

3.2 Performance of the estimation far from operating point

In order to evaluate performance of the estimation when strong changes in the unknown input are applied, disturbances to the inlet solids fraction, shown in Fig. 8, are employed. Fig. 9 shows the volumetric flow rate of slurry Q of the plant, which is represented by the continuous black line. The two estimations for this variable are represented by dashed gray and light gray lines for Options 1 and 2, respectively. According to Fig. 9, both options estimate this state without problem. Figs. 10 and 11 show the observations of ρ_2 and μ_2, respectively. The observation of both variables using both estimation options is suitable when the system is close to the steady state in which the model was linearized. However, for the second step change, a stationary state error appears in the estimation of ρ_2 using both options. This stationary state error is propagated for the observation of μ_2 using Option 2, causing the whole estimator to fail. On the other hand, for Option 1 the observation of μ_2 is close to the plant value. The effect of noise and the error propagation on Option 2 is higher than its effect on Option 1,

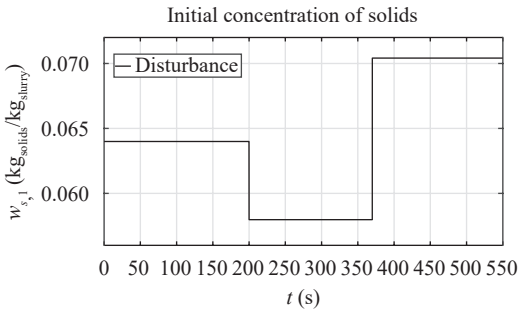

Fig. 8 Disturbances applied to the inlet solids fraction to evaluate performance of the estimation far from operating point

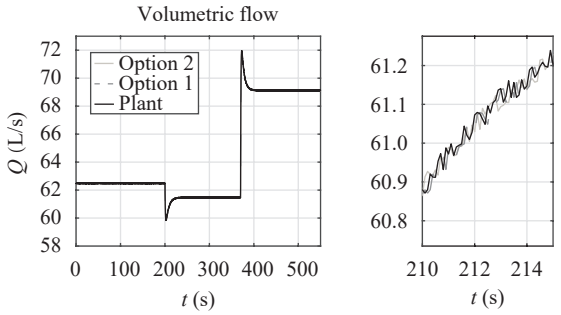

Fig. 9 Estimation of the volumetric flow of the mineral slurry considering higher disturbances in the solid concentration. Left: Volumetric flow observation using both estimation options and considering the disturbances applied to the inlet solids fraction shown in Fig. 8. The continuous black line represents the Q value of the plant. Dashed gray and light gray lines represent the estimation value of Q for Options 1 and 2, respectively. Right: Close up of left figure for $t \in [210\text{ s}, 215\text{ s}]$.

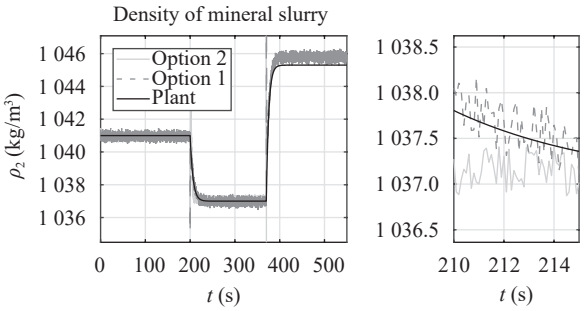

Fig. 10 Estimation of the density of the mineral slurry considering higher disturbances in the solid concentration. Left: Density observation using both estimation options and considering the disturbances applied to the inlet solids fraction shown in Fig. 8. The continuous black line represents the ρ_2 value of the plant. Dashed gray and light gray lines represent the estimation value of ρ_2 for Options 1 and 2, respectively. Right: Close up of left figure for $t \in [210\text{ s}, 215\text{ s}]$.

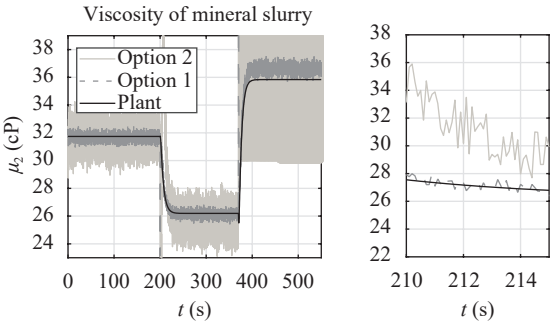

Fig. 11 Estimation of the viscosity of the mineral slurry considering higher disturbances in the solid concentration. Left: Viscosity observation using both estimation options and considering the disturbances applied to the inlet solids fraction shown in Fig. 8. The continuous black line represents the μ_2 value of the plant. Dashed gray and light gray lines represent the estimation value of μ_2 for Options 1 and 2, respectively. Right: Close up of left figure for $t \in [210\text{ s}, 215\text{ s}]$.

due to the strong dependence of Option 2 on the steady-state condition. However, note that estimation Option 1 suitably covers a wide range of viscosity observation with low error estimation.

3.3 Comparison between linear and nonlinear observers

A recent work has been developed using the nonlinear moving horizon estimator (NLMHE)[33], which is considered here to compare the performance with the estimator proposed in this work. The NLMHE employs the same nonlinear mathematical model presented in Section 2.1 with the first option for the viscosity calculation block. Therefore, we compare it to estimation Option 1, while conserving the simulation conditions. From this, the same total time of simulation, the disturbances, and the noise for the measured variable were considered. The NLMHE estimates state variables based on the online solution of an optimization problem constrained to the process model, and using a random value for the unknown input into its feasible region. Thus, the interval approach was developed by solving the proposed NLMHE both for the admissible minimum and maximum values of the unknown input, with the aim of determining the feasible region for estimation of the state variables. The admissible minimum and maximum values of the unknown input can thereby be established from the knowledge of the operating range for solids fraction, which is related to the slurry density[33].

The simulation results obtained for the estimation Option 1 and the NLMHE are shown in Figs. 12–14. According to the obtained results, the NLMHE shows an improvement in the online estimation of ρ_2 and μ_2 when the plant moves away from the steady state over which the linear observer was linearized. However, the implementation of the online optimizer in the real plant in Colombia, where the estimation is required, reduces the applicability of the NLMHE. Additionally, significant changes in operational conditions are not expected in normal plant operations.

In that sense, and given the current state of majority of industrial plants, the applicability of any soft sensor for unmeasured process variables must be discussed. The main interest for this kind of application will be for medium and small size enterprises in particular. This discussion is not about big corporations, which have a large enough instrumentation budget to install high capability computers for process control. In contrast, medium and small enterprises normally have low cost programmable logic controllers (PLCs) for data processing and control tasks. A PLC is used as a local control system for each process equipment. A medium to low cost PLC for computing equipment has limited capability for solving mathematical systems. In addition, any online optimization task assigned to this kind of PLC must be programmed as an extra module, sometimes using non-native software. Obviously, this dedicated module is an extra cost and re-

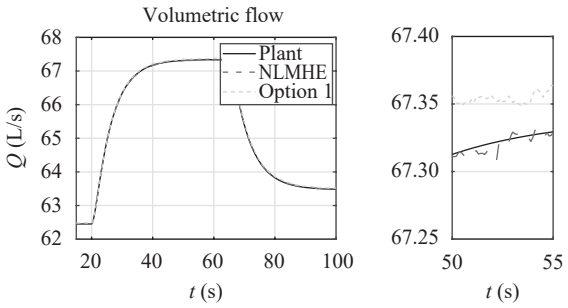

Fig. 12 Comparison of the volumetric flow estimation using the linear estimator and NLMHE. Left: Volumetric flow observation using the NLMHE[33], represented by dashed gray line, and estimation Option 1 developed in this work, represented by light gray line. The continuous black line represents the Q value of the plant. Right: Close up of left figure for $t \in [50\text{ s}, 55\text{ s}]$ where the plant moves away from the steady state over which the linear observer was linearized.

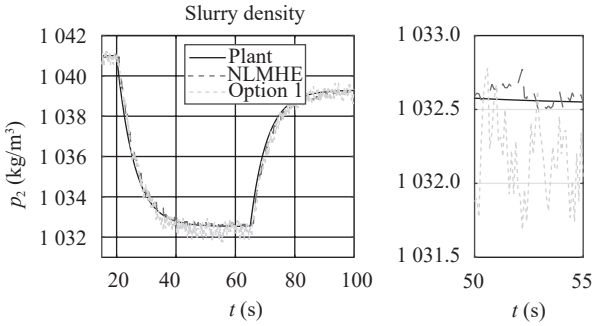

Fig. 13 Comparison of the density estimation using the linear estimator and NLMHE. Left: Density observation using the NLMHE[33], represented by a dashed gray line, and estimation Option 1 developed in this work, represented by a light gray line. The continuous black line represents the ρ_2 value of the plant. Right: Close up of left figure for $t \in [50\text{ s}, 55\text{ s}]$ where the plant moves away from the steady state over which the linear observer was linearized.

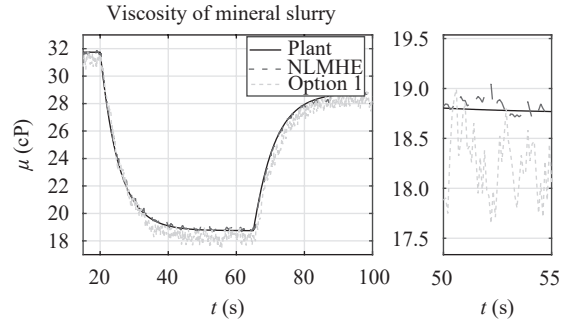

Fig. 14 Comparison of the viscosity estimation using the linear estimator and NLMHE. Left: Viscosity observation using the NLMHE[33], represented by a dashed gray line, and estimation Option 1 developed in this work, represented by a light gray line. The continuous black line represents the μ_2 value of the plant. Right: Close up of left figure for $t \in [50\text{ s}, 55\text{ s}]$ where the plant moves away from the steady state over which the linear observer was linearized.

quires specialized technicians for its programming and maintenance. Therefore, the ideal soft sensor is one with only algebraic operations to solve, hopefully without iterative processes. With these requirements, it is evident that the estimators presented here have direct application in a PLC platform for small and medium size enterprises. Our proposals require only algebraic operation and can be easily discretized without significant losses in precision.

4 Conclusions

Two different structures for the online estimation of the density and viscosity of slurries flowing through a pipe-and-fittings assembly (PFA) were developed. These approaches allowed online estimation of slurry density and viscosity, without intervening or changing the pipeline, providing a soft sensor which used only pre-installed meters. Both estimator proposals considered the use of a phenomenological based semi-physical model as the main element for estimation structure. In addition, the necessary conditions to for designing the observers were provided, with two options for viscosity computation. Although the first option was developed for the transport process of a specific slurry, it can be adjusted for other kinds of slurries, provided enough data from the laboratory is available. The second option is a more general tool because it uses the static verification of mechanical energy balance to estimate viscosity, without using exhaustive experimental information. However, the second option for prediction is poor during transitory states, which fortunately take a short time in slurry transport. In order to improve the above results, a nonlinear observer has been developed considering the unknown input as a random value[33]. Although these results show a better estimation considering disturbances that carried the system to another stationary state, the nonlinear estimation stated as a nonlinear optimization problem requires a more complicated implementation compared to the linear observers developed in this work.

Acknowledgments

The authors thank Colciencias and SUMICOL (Suministros de Colombia S.A.) for their support and financing for this project.

References

[1] M. C. Bourne. Texture, viscosity, and food. *Food Texture and Viscosity: Concept and Measurement*, 2nd ed., M. C. Bourne, Ed., London, UK: Academic Press, pp. 1–32, 2002. DOI: 10.1016/B978-012119062-0/50001-2.

[2] R. J. Oglesby, H. J. Moynihan, R. B. Santos, A. Ghosh, P. W. Hart. Does kraft hardwood and softwood pulp viscosity correlate to paper properties? *Tappi Journal*, vol. 15, no. 10, pp. 643–651, 2016.

[3] S. Taborda, D. A. Muñoz, H. Alvarez. Snowball effect detection and control proposal for its correction. In *Proceedings of IEEE Conference on Control Applications*, IEEE, Buenos Aires, Argentina, pp. 1173–1178, 2016. DOI: 10.1109/CCA.2016.7587965.

[4] W. Whiten, P. Steffens, J. Hitchins. An examination of pulp viscosity in tubes at higher shear rates. *Minerals Engineering*, vol. 6, no. 4, pp. 397–404, 1993. DOI: 10.1016/0892-6875(93)90018-I.

[5] F. N. Shi, T. J. Napier-Munn. Effects of slurry rheology on industrial grinding performance. *International Journal of Mineral Processing*, vol. 65, no. 3–4, pp. 125–140, 2002. DOI: 10.1016/S0301-7516(01)00060-6.

[6] M. C. Bourne. Viscosity measurement. *Food Texture and Viscosity*, 2nd ed., M. C. Bourne, Ed., London, UK: Academic Press, pp. 235–256, 2002. DOI: 10.1016/B978-012119062-0/50006-1.

[7] Y. Fangary, A. S. A. Ghani, S. M. El Haggar, R. A. Williams. The effect of fine particles on slurry transport processes. *Minerals Engineering*, vol. 10, no. 4, pp. 427–439, 1997. DOI: 10.1016/S0892-6875(97)00019-8.

[8] M. Z. He, Y. M. Wang, E. Forssberg. Slurry rheology in wet ultrafine grinding of industrial minerals: A review. *Powder Technology*, vol. 147, no. 1–3, pp. 94–112, 2004. DOI: 10.1016/j.powtec.2004.09.032.

[9] M. J. Tippett, J. Bao. Distributed control of chemical process networks. *International Journal of Automation and Computing*, vol. 12, no. 4, pp. 368–381, 2015. DOI: 10.1007/s11633-015-0895-9.

[10] R. P. Chhabra, J. F. Richardson. Rheometry for non-Newtonian fluids. *Non-Newtonian Flow and Applied Rheology: Engineering Applications*, 2nd ed., R. P. Chhabra, J. F. Richardson, Eds., Oxford, UK: Butterworth-Heinemann, pp. 56–109, 2008. DOI: 10.1016/B978-0-7506-8532-0.00002-0.

[11] D. Hodouin. Methods for automatic control, observation, and optimization in mineral processing plants. *Journal of Process Control*, vol. 21, no. 2, pp. 211–225, 2011. DOI: 10.1016/j.jprocont.2010.10.016.

[12] D. Sbárbaro, R. Del Villar. *Advanced Control and Supervision of Mineral Processing Plants*, London, UK: Springer, 2010. DOI: 10.1007/978-1-84996-106-6.

[13] K. M. Hangos, I. T. Cameron. *Process Modelling and Model Analysis*, San Diego, USA: Academic Press, 2001.

[14] E. Hoyos, D. López, H. Alvarez. A phenomenologically based material flow model for friction stir welding. *Materials & Design*, vol. 111, pp. 321–330, 2016. DOI: 10.1016/j.matdes.2016.09.009.

[15] R. B. Bird. *Transport Phenomena*, Sterling Heights, USA: Wiley, 2007.

[16] R. Darby. *Chemical Engineering Fluid Mechanics*, 2nd ed., New York, USA: Marcel Dekker, 2001.

[17] I. Govender, G. B. Tupper, A. N. Mainza. Towards a mechanistic model for slurry transport in tumbling mills. *Minerals Engineering*, vol. 24, no. 3–4, pp. 230–235, 2011. DOI: 10.1016/j.mineng.2010.08.010.

[18] D. Muñoz, J. L. Diaz, S. Taborda, H. Alvarez. Hydrocyclone phenomenological-based model and feasible opera-

tion region. *International Journal of Mining, Materials, and Mechanical Engineering*, vol. 3, pp. 1–9, 2017.

[19] K. J. Astrom, B. Wittenmark, *Computer-controlled Systems: Theory and Design*, 3rd ed., Berlin, Germany: Prentice Hall, 1997.

[20] M. Darouach, M. Zasadzinski, S. J. Xu. Full-order observers for linear systems with unknown inputs. *IEEE Transactions on Automatic Control*, vol. 39, no. 3, pp. 606–609, 1994. DOI: 10.1109/9.280770.

[21] M. Roco, C. A. Shook. Modeling of slurry flow: The effect of particle size. *The Canadian Journal of Chemical Engineering*, vol. 61, no. 4, pp. 494–503, 1983. DOI: 10.1002/cjce.5450610402.

[22] C. F. Ihle, A. Tamburrino. Uncertainties in key transport variables in homogeneous slurry flows in pipelines. *Minerals Engineering*, vol. 32, pp. 54–59, 2012. DOI: 10.1016/j.mineng.2012.03.002.

[23] H. Alvarez, R. Lamanna, P. Vega, S. Revollar. Methodology for obtaining phenomenological based semiphysical models applied to a sugar cane juice tower. *Iberoamericana Journal of Automation and Industrial Information*, vol. 6, no. 3, pp. 117–122, 2009.

[24] D. Castañeda, J. Lorena. The Use of Phenomenological Based Semi-physical Models as Virtual Sensors for Density and Viscosity of Mineral Slurries, Master dissertation, Facultad de Minas, Universidad Nacional de Colombia, Colombia, 2017.

[25] W. B. Hooper. The two-K method predicts head losses in pipe fittings. *Chemical Engineering*, vol. 88, pp. 96–100, 1981.

[26] B. J. Schorle, S. W. Churchill, M. Shacham. Comments on: "An explicit equation for friction factor in pipe". *Industry & Engineering Chemistry Fundamentals*, vol. 19, no. 2, pp. 228, 1980. DOI: 10.1021/i160074a019.

[27] G. Besancon. *Nonlinear Observers and Applications*, Berlin, Heidelberg Germany: Springer, 2007. DOI: 10.1007/978-3-540-73503-8.

[28] J. Garcia-Tirado, H. Botero, F. Angulo. A new approach to state estimation for uncertain linear systems in a moving horizon estimation setting. *International Journal of Automation and Computing*, vol. 13, no. 6, pp. 653–664, 2016. DOI: 10.1007/s11633-016-1015-1.

[29] K. Hfaïedh, K. Dahech, T. Damak. A sliding mode observer for uncertain nonlinear systems based on multiple models approach. *International Journal of Automation and Computing*, vol. 14, no. 2, pp. 202–212, 2017. DOI: 10.1007/s11633-016-0970-x.

[30] G. F. Aguilera. Mineral slurry viscosity simulation using neural networks, Master dissertation, Facultad de Minas, Universidad Nacional de Colombia, Colombia, 2005. [Online], Available: http://intranet.minas.medellin.unal.edu.co/index.php?option=com_docman&taskdoc_download&gid=986&Itemid=285.

[31] K. Madlener, B. Frey, H. K. Ciezki. Generalized Reynolds number for non-Newtonian fluids. *Progress in Propulsion Physics*, vol. 1, pp. 237–250, 2009. DOI: 10.1051/eucass/200901237.

[32] D. A. Muñoz, C. J. L. Diaz, H. Alvarez. Unknown input observer to estimate slurry rheological properties. In *Proceedings of the 3rd Colombian Conference on Automatic Control*, IEEE, Cartagena, Colombia, 2017. DOI: 10.1109/CCAC.2017.8276418.

[33] J. L. Diaz C, C. Ocampo-Martinez, H. Alvarez. Nonlinear moving horizon estimator for online estimation of the density and viscosity of a mineral slurry. *Industrial & Engineering Chemistry Research*, vol. 56, no. 49, pp. 14592–14603, 2017. DOI: 10.1021/acs.iecr.7b04393.

Jenny L. Diaz C. received the B. Sc. degree in chemical engineering and the M. Sc. degree in engineering with an emphasis on chemical engineering from Universidad Nacional de Colombia, Colombia in 2014 and 2016, respectively. Currently, she is a Ph. D. degree candidate in automatic at Universitat Politcnica de Catalunya, Spain.

Her research interests include modeling of chemical processes, estimation and control theory and large-scale systems management.

E-mail: jdiaz@iri.upc.edu (Corresponding author)
ORCID iD: 0000-0002-7863-4914

Diego A. Muñoz received the B. Sc. degree in chemical engineer from Universidad Nacional de Colombia, Colombia in 2004, the M. Sc. degree in mathematics from Universidad Nacional de Colombia, Colombia in 2006, and the Ph. D. degree in engineering from RWTH Aachen University of Technology, Germany in 2015. Currently he holds a full professor position at Engineering School, Universidad Pontificia Bolivariana, Venezuela, performing both research activities and teaching in the undergraduate and graduate programs.

His research interests include process optimization, modelling and control.

E-mail: diego.munoz@upb.edu.co
ORCID iD: 0000-0002-6727-6568

Hernan Alvarez received the B. Sc. degree in chemical engineer from Universidad Nacional de Colombia, Colombia in 1991, the M. Sc. degree in Systems Engineering from the Universidad Nacional de Colombia, Colombia in 1995, and the Ph. D. degree in control systems engineering from Instituto de Automática of Universidad Nacional de San Juan, Argentina in 2000. Currently, he holds a full professor position at Faculty of Mines, Processes and Energy School, Universidad Nacional de Colombia, performing both research activities and teaching in the undergraduate and graduate programs.

His research interests include chemical process modelling and control.

E-mail: hdalvare@unal.edu.co
ORCID iD: 0000-0002-2253-3583